Excited fermions and low-energy parity-violating phenomena

R. G. Ellis, M. Matsuda,* and B. H. J. McKellar
School of Physics, University of Melbourne, Parkville, Victoria 3052, Australia
(Received 28 May 1985)

A calculation is made of the parity-violating contributions of hypothetical excited quarks and leptons to two examples of low-energy phenomena. In particular, the contributions to polarized-electron—deuteron scattering and the parity-violating nuclear potential are studied. The parity-violating contributions are induced by the magnetic coupling of photons or gluons with virtual excited fermions and left-handed ordinary fermions. It is concluded that the mass of an excited quark, if it exists, must be larger than ~ 3 TeV. The restriction on the mass of an excited lepton is less stringent.

I. INTRODUCTION

The remarkable success of the Glashow-Salam-Weinberg (GSW) theory[1] is the discovery at the CERN $p\bar{p}$ collider[2] of the $W^{\pm}$ and Z bosons with masses in the predicted range. However, various anomalous events[3] are observed which suggest that the standard $SU(2)\times U(1)$ theory might not be the complete theory. These events are possibly the first indication of new physics beyond the standard model. In fact, some authors[3,4] postulate that the anomalous $l\bar{l}\gamma$ and monojet events result from excited quarks (q^*) and leptons (l^*) as a manifestation of composite fermions.

If excited fermions exist they will have consequences, albeit small, for the low-energy phenomenology.[5–8] Conversely, the low-energy phenomenology can be used to constrain the parameters of an excited-fermion Lagrangian. Hereafter, we concentrate on the constraints imposed by the low-energy parity-violating phenomena on hypothetical excited quarks and leptons.

We begin by discussing the electron-quark parity-violating interaction Lagrangian and consider the constraints imposed by the experimental results from $\vec{e}d$ scattering. In the second half of the paper we turn to the four-quark parity-violating interaction Lagrangian and use the experimental results on the parity-violating component of the nuclear force to further constrain the Lagrangian. Finally, we conclude by summarizing our results.

II. THE PARITY-VIOLATING ELECTRON-QUARK INTERACTION

Following De Rújula, Maiani, and Petronzio[4] and Cabibbo, Maiani, and Srivastava[4] we assume the following interaction Lagrangian for l^* and q^* with an ordinary electron (l) or quark (q) via a photon or gluon:

$$L=-\frac{ef}{M_{e^*}}\bar{e}^*\sigma_{\mu\nu}k^{\nu}e_L A^{\mu}+\frac{efQ_q}{M_{q^*}}\bar{q}^*\sigma_{\mu\nu}k^{\nu}q_L A^{\mu}+\frac{g_s f_s}{M_{q^*}}\bar{q}^*\sigma_{\mu\nu}k^{\nu}\frac{\lambda^i}{2}q_L G^{\mu i}+\text{H.c.}\,, \qquad (1)$$

where g_s is the strong coupling, $-e$ is the electron charge, f_s (f) is a strong (electromagnetic) moment, and $Q_q e$ is the quark charge. Also

$$q_L\equiv\begin{bmatrix}u_L\\ d_L\end{bmatrix},\quad q^*\equiv\begin{bmatrix}u^*\\ d^*\end{bmatrix}.$$

We ignore Cabibbo mixing and concentrate only on the first generation. Furthermore we ignore the contribution, from the massive gauge bosons, $W^{\pm}$ and Z because in general their contributions will be suppressed. Our motivation for ignoring these small effects is that the experimental data with which we finally compare has large uncertainties making a leading-order calculation sufficient. The parity-violating interaction between electrons and quarks is generated to lowest order by the well-known penguin diagrams and box diagrams of Fig. 1. Using Eq. (1) we obtain

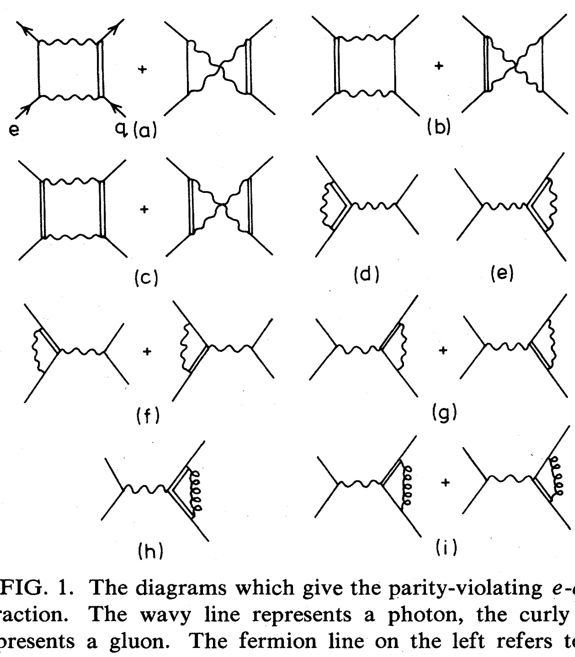

FIG. 1. The diagrams which give the parity-violating e-q interaction. The wavy line represents a photon, the curly line represents a gluon. The fermion line on the left refers to an electron while the fermion line on the right refers to a quark.

$$L=\frac{G_F}{\sqrt{2}}\alpha^2 Q_q{}^2\left[\frac{fM_W}{gM_{e^*}}\right]^2\bar{e}\gamma_\mu(f_V+f_A\gamma_5)e$$
$$\times\bar{q}\gamma^\mu(g_V+g_A\gamma_5)q\ , \tag{2}$$

where g is the SU(2) coupling constant and the coefficients $f_V g_V$, $f_V g_A$, $f_A g_V$, $f_A g_A$ are given in Table I for each diagram in Fig. 1. In this calculation we use form factors,

$$F_e(p^2)=\frac{\Lambda_e{}^2}{\Lambda_e{}^2-p^2}\ ,\ F_q(p^2)=\frac{\Lambda_q{}^2}{\Lambda_q{}^2-p^2}$$

at the e^*-e-boson and q^*-q-boson vertices to cure the nonrenormalizability of the theory. For simplicity we take $\Lambda_e=M_{e^*}$ and $\Lambda_q=M_{q^*}$ since we expect the compositeness scale $\Lambda_{e,q}$ to be of the same order as the excited fermion scale M_{e^*,q^*}.

III. POLARIZED-ELECTRON DEUTERON SCATTERING

The results of Sec. II can be applied to the low-energy phenomenology to obtain constraints on the ratios M_{e^*}/f and M_{q^*}/f. As is well known, low-energy neutral-current phenomena are well reproduced by the standard model[9] which includes only one parameter, $\sin^2\theta_W$. The value of $\sin^2\theta_W$ is usually given by the combination of various experiments. However, the existence of excited fermions, for example, could be one source of possible discrepancy between the values of $\sin^2\theta_W$ found in different experiments. In particular, $\sin^2\theta_W$ determined from the M_Z/M_W mass ratio measured at the CERN $p\bar{p}$ collider might differ from $\sin^2\theta_W$ determined from polarized-electron—deuteron scattering. Conversely, the extent to which $\sin^2\theta_W$ from various experiments agree can be used to constrain the ratios M_{e^*}/f or M_{q^*}/f in Eq. (1). We now proceed to calculate these constraints assuming that the hypothetical excited fermions are the sole source of any discrepancy in $\sin^2\theta_W$.

In polarized-electron—deuteron scattering the asymmetry parameter, A, is defined by

$$A=\frac{\sigma_R-\sigma_L}{\sigma_R+\sigma_L}=k^2a_1-k^2a_2\left[\frac{1-(1-y)^2}{1+(1-y)^2}\right]\ ,\ k^2>0 \tag{3}$$

where y is the fraction of the incident electron energy lost, and, a_1 and a_2 are given in the GSW theory by

$$a_1^{\rm GSW}=\frac{G_F}{\sqrt{2}}\left[\frac{-1}{2\pi\alpha}\frac{9}{10}(1-\tfrac{20}{9}\sin^2\theta_W)\right]\ ,$$
$$a_2^{\rm GSW}=\frac{G_F}{\sqrt{2}}\left[\frac{-1}{2\pi\alpha}\frac{9}{10}(1-4\sin^2\theta_W)\right]\ , \tag{4}$$

on the other hand, $\vec{e}d$ scattering experiments[10] give

$$a_1^{\rm expt}=(-9.7\pm2.6)\times10^{-5}\ {\rm GeV}^{-2}\ ,$$
$$a_2^{\rm expt}=(4.9\pm8.1)\times10^{-5}\ {\rm GeV}^{-2}\ . \tag{5}$$

TABLE I. The coefficients for the e-q Lagrangian, Eq. (2), for each diagram in Fig. 1.

Diagram	$g_V f_V$	$g_V f_A$	$g_A f_V$	$g_A f_A$
1(a)	0	$-6\left[\frac{M_{e^*}}{M_{q^*}}\right]^2$	0	$6\left[\frac{M_{e^*}}{M_{q^*}}\right]^2$
1(b)	0	0	-6	6
1(c)	$-\frac{4}{5}f^2\frac{M_{e^*}}{M_{q^*}}$	$\frac{4}{5}f^2\frac{M_{e^*}}{M_{q^*}}$	$\frac{4}{5}f^2\frac{M_{e^*}}{M_{q^*}}$	$-\frac{4}{5}f^2\frac{M_{e^*}}{M_{q^*}}$
1(d)	$\frac{89}{360}\frac{1}{Q_q}$	$-\frac{89}{360}\frac{1}{Q_q}$	0	0
1(e)	$\frac{89}{360}Q_q\left[\frac{M_{e^*}}{M_{q^*}}\right]^2$	0	$-\frac{89}{360}Q_q\left[\frac{M_{e^*}}{M_{q^*}}\right]^2$	0
1(f)	$-6\frac{1}{Q_q}$	$6\frac{1}{Q_q}$	0	0
1(g)	$-6Q_q\left[\frac{M_{e^*}}{M_{q^*}}\right]^2$	0	$6Q_q\left[\frac{M_{e^*}}{M_{q^*}}\right]^2$	0
1(h)	$\frac{89}{360}\frac{\alpha_s}{\alpha}\frac{1}{Q_q}\left[\frac{f_sM_{e^*}}{fM_{q^*}}\right]^2$	0	$-\frac{89}{360}\frac{\alpha_s}{\alpha}\frac{1}{Q_q}\left[\frac{f_sM_{e^*}}{fM_{q^*}}\right]^2$	0
1(i)	$-8\frac{\alpha_s}{\alpha}\frac{1}{Q_q}\frac{f_s}{f}\left[\frac{M_{e^*}}{M_{q^*}}\right]^2$	0	$8\frac{\alpha_s}{\alpha}\frac{1}{Q_q}\frac{f_s}{f}\left[\frac{M_{e^*}}{M_{q^*}}\right]^2$	0

We use the value of $\sin^2\theta_W$ independently given by the CERN $p\bar{p}$ collider[11] from the M_Z/M_W mass ratio,

$$\sin^2\theta_W = 0.243 \pm 0.030 \tag{6}$$

and argue that the contribution to a_1 and a_2 from e^* and q^* effects, denoted a_1^* and a_2^* must be less than any discrepancy between the GSW theory with the CERN $\sin^2\theta_W$ as input and the $\vec{e}d$ experimental result or at least within the associated errors, i.e.,

$$\begin{aligned} &-5.9\times10^{-5} \lesssim a_1^* \lesssim 1.4\times10^{-5} ; \\ &-4.7\times10^{-5} \lesssim a_2^* \lesssim 1.5\times10^{-4} . \end{aligned} \tag{7}$$

Using the results of Table I we find for the excited-fermion contributions,

$$a_1^* = \frac{\alpha}{\pi}\frac{G_F}{\sqrt{2}}\frac{7}{10}\left[-\frac{2071}{504}\delta^2 - \frac{4}{15}\delta\beta f^2 + 2\beta^2\right] , \tag{8}$$

$$\begin{aligned} a_2^* = \frac{\alpha}{\pi}\frac{G_F}{\sqrt{2}}\frac{9}{10}\Bigg[&\frac{35207}{29160}\beta^2 + \frac{28}{135}\delta\beta f^2 - \frac{14}{9}\delta^2 \\ &- \frac{89}{486}\frac{\alpha_s}{\alpha}\gamma^2 + \frac{40}{9}\frac{\alpha_s}{\alpha}\beta\gamma \Bigg] , \end{aligned} \tag{9}$$

where

$$\beta = \frac{f}{g}\frac{M_W}{M_{q^*}} , \quad \gamma = \frac{f_s}{g}\frac{M_W}{M_{q^*}} , \quad \delta = \frac{f}{g}\frac{M_W}{M_{e^*}}$$

and $\alpha_s = \alpha_s(M_{q^*}^2)$. To overcome the dependence of α_s on M_{q^*} it is simplest to input some values of M_{q^*} and finally check for consistency. We take $M_{q^*} = 0.1$TeV and 10 TeV and $\alpha_s((0.1\text{ TeV})^2) = 0.17$, $\alpha_s((10\text{ TeV})^2) = 0.09$.

Given the rather weak constraints on a_1^* and a_2^* in Eq. (7) it is consistent to make the reasonable and simplifying assumptions that $f/M_{l^*} \simeq f_s/M_{q^*} \simeq f/M_{q^*}$ and $f \sim 1$. Under these assumptions Eq. (8) together with Eq. (7) gives

$$\begin{aligned} &\frac{M_{q^*}}{f_s} \sim \frac{M_{q^*}}{f} \gtrsim 13\text{ GeV} , \quad \frac{M_{e^*}}{f} \gtrsim 4\text{ GeV} , \\ &\qquad (M_{q^*} = 0.1\text{ TeV used as input}) , \\ &\frac{M_{q^*}}{f_s} \gtrsim \frac{M_{q^*}}{f} \gtrsim 10\text{ GeV} , \quad \frac{M_{e^*}}{f} \gtrsim 4\text{ GeV} , \\ &\qquad (M_{q^*} = 10\text{ TeV used as input}) . \end{aligned} \tag{10}$$

This is a rather weak constraint for the excited electron when compared with existing constraints from the anomalous magnetic moment of the electron[5,12] $\delta(g-2)_e$

$$\frac{M_{e^*}}{f} \gtrsim 2.6\text{ GeV} \tag{11}$$

and the deviation from QED predictions for $e^+e^- \to 2\gamma$ which gives[13]

$$\frac{M_{e^*}}{f} \gtrsim 50\text{ GeV} . \tag{12}$$

On the other hand, there is no existing rigorous restriction on the excited quark mass and coupling f_s; hence, Eq. (10) is useful in this sense. We note that the lower bound on the excited fermion masses in Eq. (10) will become more restrictive when new measurements with smaller errors are available from both $\vec{e}d$ scattering and the CERN $p\bar{p}$ collider.

A more useful restriction than Eq. (10) can be obtained for M_{q^*}/f_s from the limit on the parity-violating component of the nuclear potential, as discussed in the following sections.

IV. THE PARITY-VIOLATING EFFECTIVE FOUR-QUARK LAGRANGIAN

We now turn our attention to the purely baryonic sector, and attempt to use constraints on the parity-violating nuclear potential to find a lower bound on the excited quark mass. A similar analysis has been performed by Krawczyk[14] to place a lower bound on the gluino mass and our calculation proceeds along a similar line. We begin by deriving the effective four-quark parity-violating (EFQPV) Lagrangian resulting from virtual excited quarks. This Lagrangian then forms the basis of a parity-nonconserving contribution to the nuclear potential.

Using the qq^* gluon sector of the Lagrangian in Eq. (1) and the penguin and box diagrams shown in Fig. 2 we obtain the following EFQPV Lagrangians

$$\begin{aligned} L^8 = \frac{G_F}{\sqrt{2}}\alpha_s^2(m^2)\left[\frac{f_s M_W}{g M_{q^*}}\right]^2 &\bar{q}\gamma_\mu(g_V + g_A\gamma_5) \\ \times \frac{\vec{\lambda}^i}{2} q\bar{q}\gamma^\mu(g_V' + g_A'\gamma_5)\frac{\vec{\lambda}^i}{2}q & \end{aligned} \tag{13a}$$

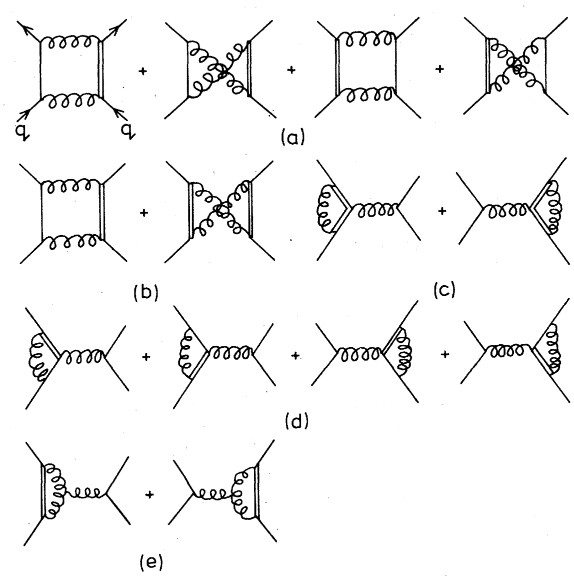

FIG. 2. The diagrams which give the parity-violating q-q interaction.

TABLE II. The coefficients for the color-octet four-quark Lagrangian, Eq. (13a), for the diagrams shown in Fig. 2.

Diagram	$g_V g_V'$	$g_V g_A'$	$g_A g_V'$	$g_A g_A'$
2(a)	$\frac{18}{4}$	$\frac{17}{4}$	$\frac{17}{4}$	$-\frac{52}{4}$
2(b)	$-\frac{21}{960}f_s^2$	$\frac{21}{960}f_s^2$	$\frac{21}{960}f_s^2$	$-\frac{21}{960}f_s^2$
2(c)	$\frac{178}{2160}\rho^2$	$-\frac{89}{2160}\rho^2$	$-\frac{89}{2160}\rho^2$	0
2(d)	$-2\rho^2$	ρ^2	ρ^2	0
2(e)	$-\frac{127}{12}\pi^2$	$\frac{127}{24}\pi^2$	$\frac{127}{24}\pi^2$	0

and

$$L^1=\frac{G_F}{\sqrt{2}}\alpha_s{}^2(m^2)\left[\frac{f_s M_W}{g M_{q^*}}\right]^2 \bar{q}\gamma_\mu(\tilde{g}_V+\tilde{g}_A\gamma_5)q$$

$$\times\bar{q}\gamma^\mu(\tilde{g}'_V+\tilde{g}'_A\gamma_5)q\ , \qquad (13b)$$

where L^8 gives the color-octet interaction, L^1 gives the color-singlet interaction, and m is the nucleon mass. The coefficient products, $g_V g_V'$, $g_V g_A'$, etc., are given in Tables II and III for L^8 and L^1, respectively. Furthermore, we have introduced[15] the parameter ρ in the excited penguin diagrams to incorporate the different energy scales, where

$$\rho^2=\frac{\alpha_s(m^2)}{\alpha_s(\text{loop})}\ . \qquad (13c)$$

We take $\alpha_s(\text{loop})\simeq\alpha_s(M_{q^*}^2)$ and $\alpha_s(m^2)\simeq 1$ which gives $\rho^2\simeq 6$, 13 for $M_{q^*}=0.1$, 10 TeV.

The EFQPV Lagrangians Eqs. (13a) and (13b) can be incorporated into the QCD environment by using the standard strong-interaction enhancement factors as first set out by Altarelli *et al.*[16] It is a simple matter to read off the strong enhancement factors[17] so that the QCD-corrected EFQPV Lagrangian becomes

$$L_{\text{PV}}=\frac{G_F}{\sqrt{2}}\alpha_s{}^2(m^2)\left[\frac{f_s M_W}{q M_{q^*}}\right]^2\left[c\bar{q}\gamma_\mu\gamma_5\frac{\vec{\lambda}^i}{2}q\bar{q}\gamma^\mu\frac{\vec{\lambda}^i}{2}q\right.$$

$$\left.+d\,\bar{q}\gamma_\mu\gamma_5 q\bar{q}\gamma^\mu q\right]\ , \qquad (14)$$

TABLE III. The coefficients for the color-singlet four-quark Lagrangian, Eq. (13b), for the diagrams shown in Fig. 2.

Diagram	$\tilde{g}_V\tilde{g}'_V$	$\tilde{g}_V\tilde{g}'_A$	$\tilde{g}_A\tilde{g}'_V$	$\tilde{g}_A\tilde{g}'_A$
2(a)	0	$-\frac{4}{3}$	$-\frac{4}{3}$	$\frac{8}{3}$
2(b)	$\frac{8}{45}$	$\frac{8}{45}$	$\frac{8}{45}$	$-\frac{8}{45}$

where

$$c=(g_A g_V'+g_V g_A')(0.53\ \mathrm{K}^{0.35}+0.46\ \mathrm{K}^{-0.40})$$
$$+(\tilde{g}_A\tilde{g}'_V+\tilde{g}_V\tilde{g}'_A)(-0.84\ \mathrm{K}^{0.35}+0.83\ \mathrm{K}^{-0.40})\ ,$$
$$d=(g_A g_V'+g_V g_A')(-0.29\ \mathrm{K}^{0.35}+0.29\ \mathrm{K}^{-0.40})$$
$$+(\tilde{g}_A\tilde{g}'_V+\tilde{g}_V\tilde{g}'_A)(0.46\ \mathrm{K}^{0.35}+0.52\ \mathrm{K}^{-0.40})\ ,$$

where

$$K=K(\nu^2)=1+\frac{\alpha_s(\mu^2)}{4\pi}b\ln\left[\frac{\nu^2}{\mu^2}\right]\ ,$$

$b=11-\frac{2}{3}N$, N is the number of quark flavors, μ^2 is the subtraction point which we take ~ 1 GeV, and ν^2 is the scale at which the approximation of the effective action by local operators fails. For example, in the GSW model considered by Altarelli *et al.*[16] $\nu^2\simeq M_W{}^2$, or in the supersymmetry model of Krawczyk[14] $\nu^2\simeq M_{\tilde{q}}{}^2$ and in our case $\nu^2\simeq M_{q^*}{}^2$. Therefore with $N=6$, $\alpha(\mu^2)\simeq 1$, $\mu^2\simeq 1$ GeV, and $M_{q^*}=0.1$ TeV we obtain $K\simeq 6$, whereas with $M_{q^*}=10$ TeV we obtain $K\simeq 11$. Thus we see that K is not very sensitive to the precise value chosen for M_{q^*}.

V. THE PARITY-VIOLATING NUCLEAR POTENTIAL

The results of Sec. III can be used to derive a parity-violating nuclear potential and by subsequently comparing with experiment we can constrain the ratio M_{q^*}/f_s.

At low energies the parity-violating nuclear potential can be described in terms of meson exchanges and has the general form[14,17]

$$\begin{aligned}V_{\text{pv}}^{12}=&\frac{f_\pi g_{\pi NN}}{\sqrt{2}}i\frac{(\tau_1\times\tau_2)^z}{2}(\sigma_1+\sigma_2)\cdot\left[\frac{\mathbf{p}_1-\mathbf{p}_2}{2m},f_\pi(r)\right]\\
&-g_\rho\left[h_\rho^0\tau_1\cdot\tau_2+h_\rho^1\left[\frac{\tau_1+\tau_2}{2}\right]^z+h_\rho^2\frac{(3\tau_1^z\tau_2^z-\tau_1\cdot\tau_2)}{2\sqrt{6}}\right]\\
&\times\left[(\sigma_1-\sigma_2)\cdot\left\{\frac{\mathbf{p}_1-\mathbf{p}_2}{2m},f_\rho(r)\right\}+i(1+\chi_V)(\sigma_1\times\sigma_2)\cdot\left[\frac{\mathbf{p}_1-\mathbf{p}_2}{2m},f_\rho(r)\right]\right]-g_\omega\left[h_\omega^0+h_\omega^1\left[\frac{\tau_1+\tau_2}{2m}\right]^z\right]\\
&\times\left[(\sigma_1-\sigma_2)\cdot\left\{\frac{\mathbf{p}_1-\mathbf{p}_2}{2m},f_\omega(r)\right\}+i(1+\chi_S)(\sigma_1\times\sigma_2)\left[\frac{\mathbf{p}_1-\mathbf{p}_2}{2m},f_\omega(r)\right]\right]\\
&-(g_\omega h_\omega^1-g_\rho h_\rho^1)\left[\frac{\tau_1-\tau_2}{2}\right]^z(\sigma_1\cdot\sigma_2)\cdot\left\{\frac{\mathbf{p}_1-\mathbf{p}_2}{2m},f_\rho(r)\right\}\\
&-g_\rho h_\rho^{1\prime}i\left[\frac{\tau_1\times\tau_2}{2}\right]^z(\sigma_1+\sigma_2)\cdot\left[\frac{\mathbf{p}_1-\mathbf{p}_2}{2m},f_\rho(r)\right]\ ,\end{aligned}\qquad (15)$$

where $f_\pi(r)=e^{-m_\pi r}/4\pi r$ and $f_\rho(r)=e^{-m_\rho r}/4\pi r$.

Unfortunately, it is not yet possible to determine all the parameters $(h_\rho^0,h_\rho^1,h_\rho^2,h_\omega^0,h_\rho^{1'})$ for several reasons. First, a theoretical calculation from the four-quark Hamiltonian is plagued with the same uncertainties involving long-distance contributions and hadronic wave-function effects which have so far prevented a totally satisfactory explanation of the nonlepton $\Delta I=\frac{1}{2}$ rule. Second, the empirical determination of the parameters is inhibited by uncertainties in the nuclear structure calculation and by the fact that the experiments themselves are difficult and have large errors in many cases, and finally, the parameters are highly correlated throughout the experiments to date. Indeed as shown by Desplanques and Missimer[18] most of the currently measured observables can be fitted by just two parameters. For our comparison with experiment we take the following experimental data:

$P_\gamma(^{18}\mathrm{F})=-(0.8\pm1.2)\times10^{-3}$, Adelberger *et al.* (Ref. 19),

$A_\gamma(^{19}\mathrm{F})=-(6.8\pm1.8)\times10^{-5}$, Elsener *et al.* (Ref. 20),

$P_\gamma(^{21}\mathrm{Ne})=(0.8\pm1.4)\times10^{-3}$, Adelberger *et al.* (Ref. 19).

The polarizations and asymmetry can be expressed in terms of the weak meson-nucleon couplings in Eq. (15) as

$$|P_\gamma(^{18}\mathrm{F})|\simeq|4180f_\pi-800h_\omega^1|\ ,$$

$$A_\gamma(^{19}\mathrm{F})\simeq-95.8f_\pi+34.6h_\rho^0+17.0h_\omega^1+19.4h_\phi^0\ ,$$

$$|P_\gamma(^{21}\mathrm{Ne})|\simeq|29\,085f_\pi+11\,617h_\rho^0-4766h_\omega^1+6851h_\omega^0|\ .$$

In these expressions the coefficients of the potential parameters are subject to uncertainties generated by our lack of knowledge of the nuclear structure. It therefore suffices to replace the four parameters f_π, h_ω^1, h_ρ^0, and h_ω^0 with two parameters X^1 and X^0 which are defined by

$$X^1=f_\pi-0.18h_\omega^1\ ,$$
$$X^0=h_\rho^0+0.58h_\omega^0\ . \tag{16}$$

A least-squares fit to the experimental data gives

$$X^1=(0.37\pm0.06)\times10^{-6}\ ,$$
$$X^0=-(0.86\pm0.15)\times10^{-6}\ . \tag{17}$$

With these values $A_\gamma^{\mathrm{fit}}(^{19}\mathrm{F})\simeq-6.5\times10^{-5}$, $|P_\gamma^{\mathrm{fit}}(^{18}\mathrm{F})|\simeq1.5\times10^{-3}$, and $|P_\gamma^{\mathrm{fit}}(^{21}\mathrm{Ne})|\simeq0.77\times10^{-3}$. Maintaining the philosophy of Sec. III we argue that the contributions to X^0 and X^1 from virtual excited quarks, denoted X_*^1 and X_*^0, must be less than the difference of the experimental values and the contribution from the GSW model, X_{GSW}^1 and X_{GSW}^0.

The calculation of Desplanques, Donoghue, and Holstein[17] gives a "reasonable range" for X_{GSW}^1 and X_{GSW}^0

$$0\lesssim X_{\mathrm{GSW}}^1\lesssim1.2\times10^{-6}\ ,$$
$$-3.6\times10^{-6}\lesssim X_{\mathrm{GSW}}^0\lesssim1.5\times10^{-6} \tag{18}$$

and also gives "best" values, $X_{\mathrm{GSWb}}^1=0.50\times10^{-6}$ and $X_{\mathrm{GSWb}}^0=1.3\times10^{-6}$. Thus for the "reasonable range,"

$$-0.9\times10^{-6}\lesssim X_*^1\lesssim0.4\times10^{-6}\ ,$$
$$-2.5\times10^{-6}\lesssim X_*^0\lesssim2.9\times10^{-6}\ ,$$

and for the "best" value,

$$-0.2\times10^{-6}\lesssim X_*^1\lesssim-0.1\times10^{-6}\ ,$$
$$-0.3\times10^{-6}\lesssim X_*^0\lesssim0.6\times10^{-6}\ . \tag{19}$$

Using L_{PV} from Eq. (14) and the approach of Ref. 17 gives

$$X_*^1=0\ ,$$
$$X_*^0=\alpha_s^2(m^2)\left[\frac{f_sM_W}{gM_{q^*}}\right]^2[a_V(0.64c+1.33d)+b_V(-1.33c+0.89d)-c_V(0.75c+3.99d)]\ , \tag{20}$$

where a_V, b_V, and c_V are related to the hyperon weak decays,[17]

$$a_V=1.9\times10^{-6}\ ,$$
$$b_V=-4.0\times10^{-6}/\mathrm{K}^{0.48}\ , \tag{21}$$
$$c_V=6.4\times10^{-6}/(\mathrm{K}^{0.48}+\mathrm{K}^{-0.24})\ .$$

We note that the values given in Eq. (21) are calculated within the GSW model and, consequently, K in Eq. (21) is really $K_{\mathrm{GSW}}=K(M_W^2)$ defined in Eq. (14). However, the dependence on arguments of K is mild and the parameter ranges in Eq. (19) are rather large so it is sufficient to simply use $K=K(M_{q^*}^2)$ everywhere. Doing this we find for the reasonable range and best value of the GSW model, respectively,

$$\frac{M_{q^*}}{f_s}\gtrsim1.5\ \text{TeV and }3.4\ \text{TeV}\quad(M_{q^*}=0.1\ \text{TeV used as input})\ ,$$
$$\frac{M_{q^*}}{f_s}\gtrsim1.6\ \text{TeV and }3.6\ \text{TeV}\quad(M_{q^*}=10\ \text{TeV used as input})\ , \tag{22}$$

where the value of M_{q^*} on the right-hand side of Eq. (22) refers to the value used in estimating ρ^2 in Eq. (13c) and K in Eqs. (14) and (21). Clearly, the final lower limit on the q^* mass is very weakly dependent on the input value of M_{q^*} and we assert that experiments measuring the parity-violating nucleon potential constrain $M_{q^*}/f_s \gtrsim 3$ TeV. This should be compared with our estimates from polarized-electron deuteron scattering, $M_{q^*}/f_s \gtrsim 10, 13$ GeV in Sec. III.

Other estimates of M_{q^*}/f_s have been made using the K_L-K_s mass difference: Senba and Tanimoto[6] find that it is unlikely that the existence of excited quarks of order 100 GeV is compatible with the K_L-K_s mass difference, while Choudhury, Ellis, and Joshi[7] find that $M_{q^*}/f_s \gtrsim 250$ GeV is compatible, and Greenberg, Mohapatra, and Nussinov[8] find that the compositeness scale could be "as low as several hundred GeV." We note that our limits are a significant improvement on these other determinations of M_{q^*}/f_s.

VI. CONCLUSION

We have studied two aspects of the low-energy parity-violating phenomena and found that the parameters in the excited-fermion Lagrangian must satisfy certain constraints if excited fermions are to exist within the framework of the present experimental data.

In particular, using polarized-electron deuteron scattering data and the CERN $p\bar{p}$ collider results we found that following the definitions of Eq. (1), $M_{e^*}/f \gtrsim 4$ GeV and $M_{q^*}/f_s \gtrsim 10$ GeV. These are rather weak constraints due to the substantial errors associated with the current measurements.

A much stronger constraint was obtained for M_q^*/f_s using limits on the parity-violating component of the nuclear potential: $M_q^*/f_s \gtrsim 3$ TeV. We believe that this is the most restrictive constraint on this ratio to date.

Future experiments at the CERN $p\bar{p}$ collider and on low-energy parity-violating phenomena will help to resolve the intriguing question, where is the compositeness scale? Our result suggests that we will have to search at least to the several TeV region to find the compositeness scale in the quark sector.

---

*Permanent address: Department of Physics, Aichi University of Education, Kariya, Aichi, Japan 448.

[1]S. L. Glashow, Nucl. Phys. **22**, 579 (1961); S. Weinberg, Phys. Rev. Lett. **19**, 1264 (1967); **27**, 1688 (1971); A. Salam, *Elementary Particle Theory: Relativistic Groups and Analyticity (Nobel Symposium No. 8),* edited by N. Svartholm (Almqvist and Wiksell, Stockholm, 1968), p. 367.

[2]UA1 Collaboration, G. Arnison *et al.* Phys. Lett. **122B**, 103 (1983); **126B**, 398 (1983); **129B**, 398 (1983). UA2 Collaboration, G. Banner *et al. ibid.* **122B**, 476 (1983); **129B** 130 (1983).

[3]L. J. Hall, R. L. Jaffe, and J. L. Rosner, CERN Report No. CERN-TH 3991/84 (unpublished), and references therein.

[4]A. De Rújula, L. Maiani, and R. Petronzio, Phys. Lett. **140B**, 253 (1984); J. Kuhn and P. Zerwas, *ibid.* **147B**, 189 (1984); V. Barger, H. Baer, and K. Hagiwara, Phys. Rev. D **30**, 1513 (1984); K. Enquist and J. Maalampi, Phys. Lett. **135B**, 329 (1984); N. Cabibbo, L. Maiani, and Y. Srivastava, *ibid.* **139B**, 459 (1984); S. R. Choudhury, R. G. Ellis, and G. C. Joshi, Phys. Rev. D **31**, 2390 (1985); S. S. Gernshtein, G. V. Jickia, and Yu. F. Pirogov, Phys. Lett. **151B**, 303 (1985).

[5]F. M. Renard, Phys. Lett. **116B**, 264 (1982); M. Suzuki, *ibid.* **143B**, 237 (1984); F. del Aguila, A. Mendez, and R. Pascual, *ibid.* **140B**, 431 (1984).

[6]K. Senba and M. Tanimoto, Phys. Lett. **150B**, 209 (1985).

[7]S. R. Choudhury, R. G. Ellis, and G. C. Joshi, Melbourne University Report No. UM-P-84/72 (unpublished).

[8]O. W. Greenberg, R. N. Mohapatra, and S. Nussinov, Phys. Lett. **148B**, 465 (1984).

[9]E. D. Commins and P. H. Bucksbaum, Ann. Rev. Nucl. Part. Sci. **30**, 1 (1980).

[10]C. Y. Prescott *et al.*, Phys. Lett. **77B**, 347 (1978).

[11]H. D. Wahl, CERN Report No. CERN-EP/84-127 (unpublished).

[12]F. Combley *et al.*, Phys. Rep. **68**, 93 (1981); and for a review of substructure effects see, e.g., L. Lyons, *Progress in Particle and Nuclear Physics,* edited by D. H. Wilkinson (Pergamon, New York, 1983), Vol. 10, p. 227.

[13]S. Yamada, in *Proceedings of the 1983 International Symposium on Lepton and Photon Interactions at High Energies, Ithaca, New York,* edited by D. G. Cassel and D. L. Kreinick (Newman Laboratory of Nuclear Studies, Cornell University, Ithaca, 1983).

[14]P. Krawczyk, CERN Report No. CERN-Th3977/84 (unpublished).

[15]M. J. Duncan, Nucl. Phys. Report No. **B214**, 21 (1983).

[16]G. Altarelli *et al.*, Nucl Phys. **B88**, 215 (1975).

[17]B. Desplanques, J. F. Donoghue, and B. R. Holstein, Ann. Phys. (N.Y.) **124**, 449 (1980); D. Desplanques, Nucl. Phys. **A335**, 147 (1980).

[18]B. Desplanques and J. Missimer, Nucl. Phys. **A300**, 286 (1978).

[19]E. G. Adelberger *et al.* Phys. Rev. Lett. **34**, 402 (1975).

[20]K. Elsener *et al.*, Institute for Medium Energy Physics, Eidgenössische Technische Hochschule, Hönggerberg, Zürich Report, 1985 (unpublished).